

Supplementary Information

Temperature-induced mobility in Octacalcium Phosphate impacts crystal symmetry: water dynamics studied by NMR crystallography

Adam Nelson,^{1,2} Wassilios Papawassiliou,³ Subhradip Paul,³ Sabine Hediger,³ Ivan Hung,⁴ Zhehong Gan,⁴ Amrit Venkatesh,⁴ W. Trent Franks,⁵ Mark E. Smith,^{5,6} David Gajan,⁷ Gaël De Paëpe,³ Christian Bonhomme,¹ Danielle Laurencin,^{2,*} Christel Gervais^{1,*}

¹ LCMCP, UMR 7574, Sorbonne Université, CNRS, Paris, France

² ICGM, Univ Montpellier, CNRS, ENSCM, Montpellier, France

³ IRIG, MEM, Univ. Grenoble Alpes, CEA, CNRS, 38000 Grenoble, France

⁴ National High Magnetic Laboratory (NHMFL), Tallahassee, Florida, USA

⁵ Department of Physics, University of Warwick, Coventry, CV4 7AL, UK

⁶ Department of Chemistry, University of Southampton, SO17 1BJ, UK

⁷ CRMN Lyon, UMR 5082 (CNRS, ENS Lyon, Université Lyon 1), Villeurbanne, France

christel.gervais_stary@sorbonne-universite.fr

danielle.laurencin@umontpellier.fr

Figure S1: ^{31}P CPMAS NMR spectra of the unenriched OCP sample ($B_0 = 9.4$ T, $\nu_r = 10$ kHz) recorded at ca. 100 K under DNP conditions, with (red) or without (blue) microwave irradiation suitable for DNP. The latter spectrum was scaled to four time its intensity. The measured $\varepsilon_{\text{on/off}}$ enhancement in this configuration is 29.

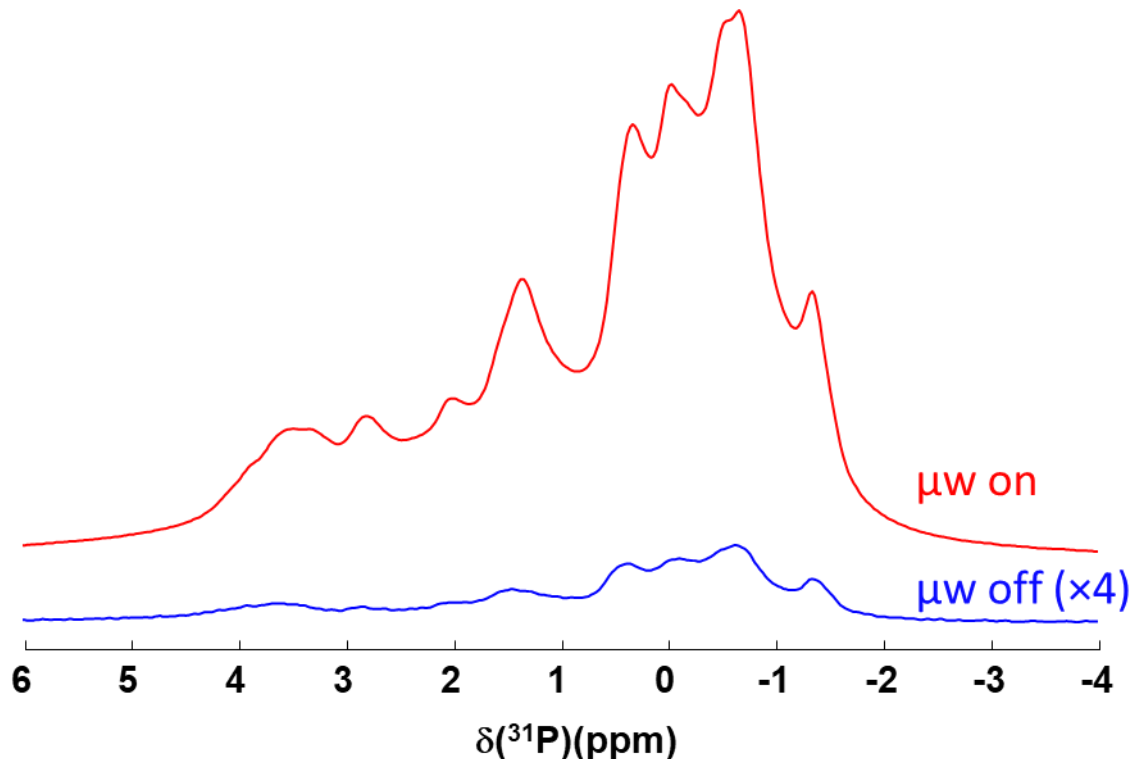


Figure S2: a) pXRD patterns of samples synthesized using the different protocols described in this study. Patterns are scaled here so that the higher intensity diffraction peaks of OCP are compared (implying a “truncation” of the lowest diffraction peak of OCP, at ca 4.7 °). The simulated pXRD pattern of OCP (starting from the experimental .cif file ICSD 65347) is shown in dark grey at the top. b) ATR-IR transmission spectra of the different samples, scaled to match intensities. Magnified below is a comparison of the same spectra, highlighting the strong P-O stretching bands around 1020 cm^{-1} , and showing clear evidence of shifting due to the increased mass of the oxygen isotopes in the enriched samples (with, as expected, more significant shifts upon ^{18}O -labeling compared to ^{17}O -labeling). Because the enrichment is only partial (theoretically, ca. 40%), there are overlaps between resonances belonging to different oxygen isotopes, leading to a loss of resolution on the IR spectra.

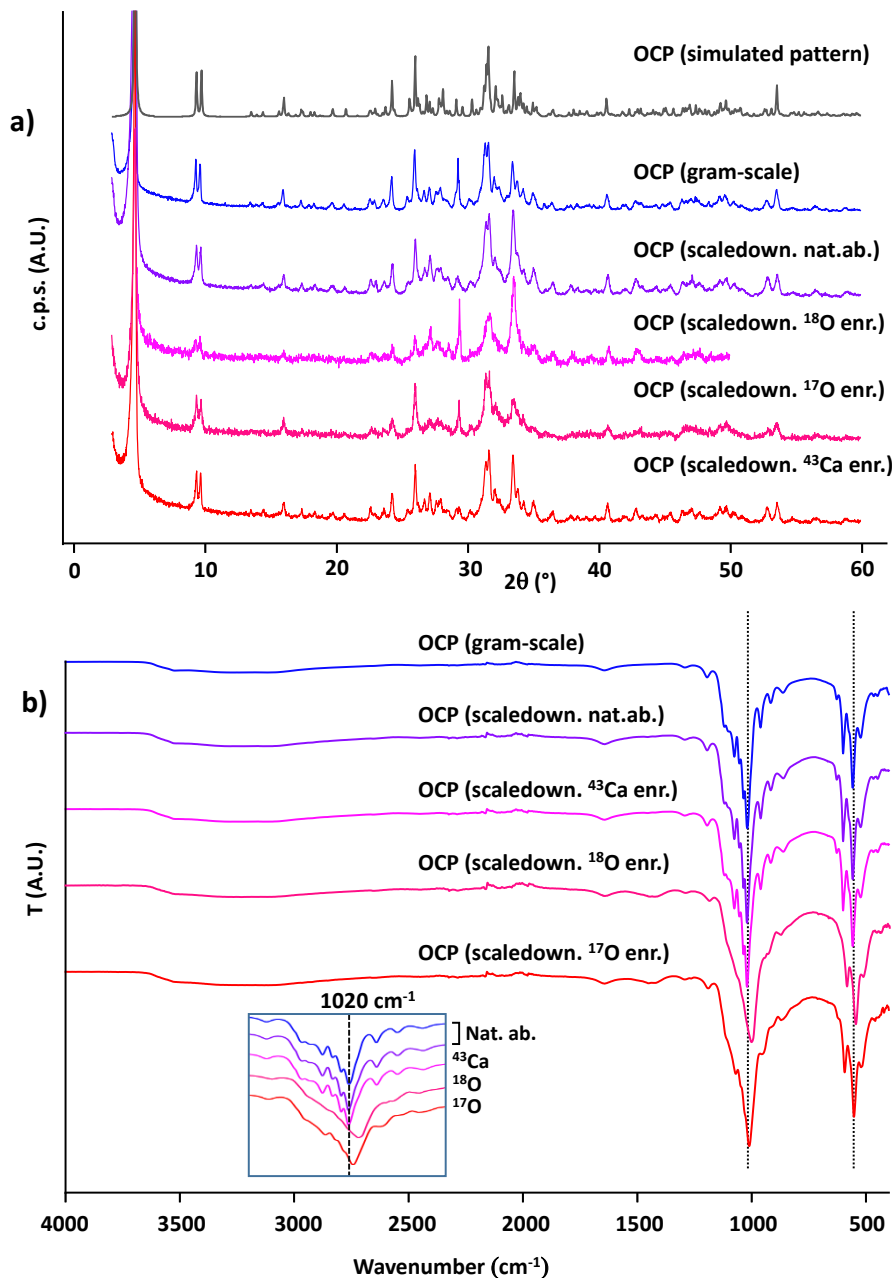


Figure S3: a) SEM images of OCP particles. b) TEM images of OCP crystallites, obtained at natural-abundance with the two protocols described in this work. c) ^{31}P CPMAS NMR spectra ($B_0 = 14.1\text{ T}$, $v_r = 20\text{ kHz}$, $t_{\text{CP}} = 1\text{ ms}$, refrigerating unit set to $0\text{ }^\circ\text{C}$) of three OCP samples. The couplings between the ^{17}O and ^{31}P isotopes are visible from the splittings observed for the ^{17}O -enriched sample.

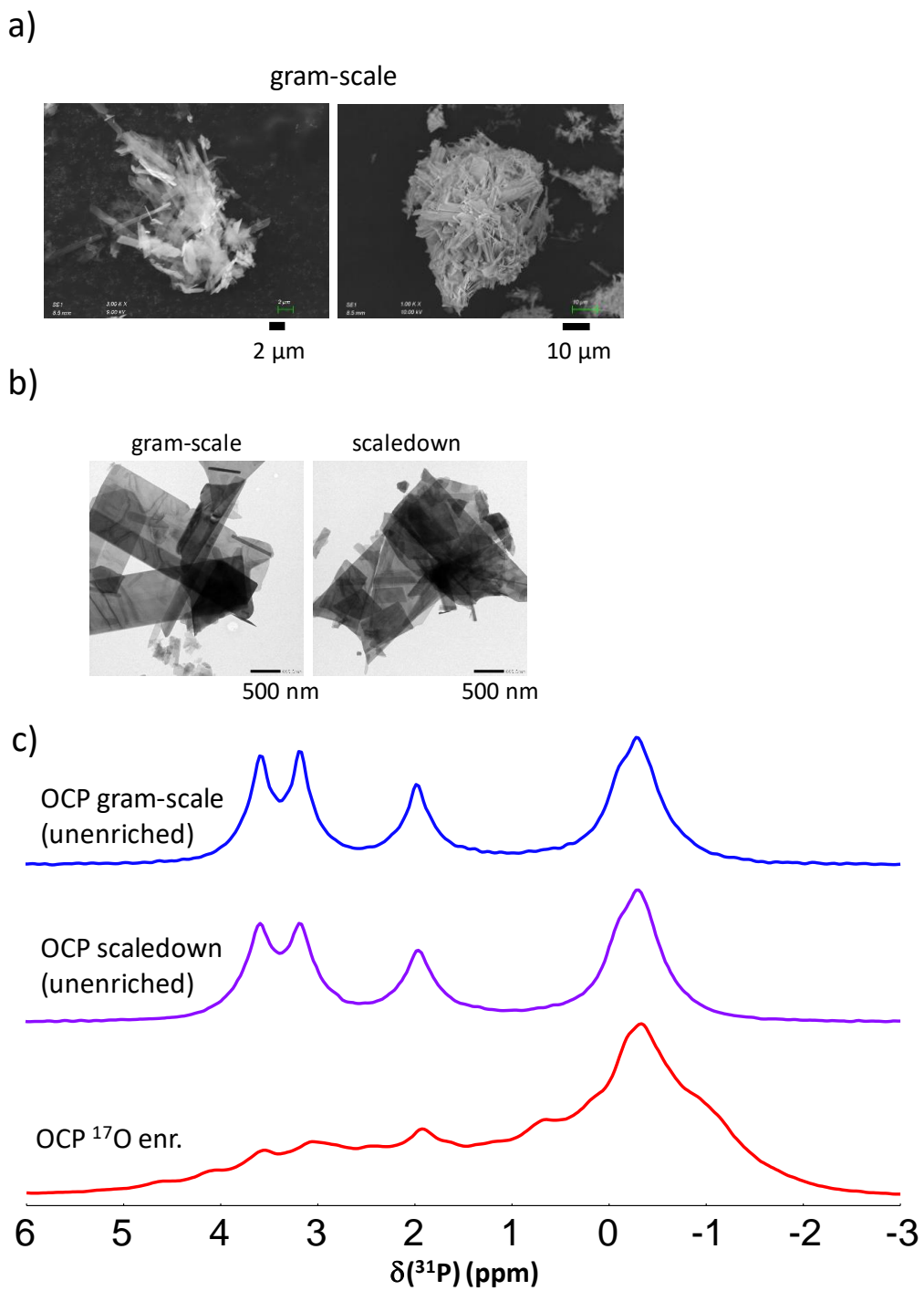


Figure S4: Experimental ^{17}O Hahn-Echo MAS NMR spectra of OCP recorded at ambient temperature:
a) $B_0 = 35.2$ T, $v_r = 25$ kHz b) $B_0 = 18.8$ T, $v_r = 25$ kHz (in black). A tentative fit is shown below each spectrum, with individual contributions of the PO and P-OH sites in blue, and their sum in red dashed line.

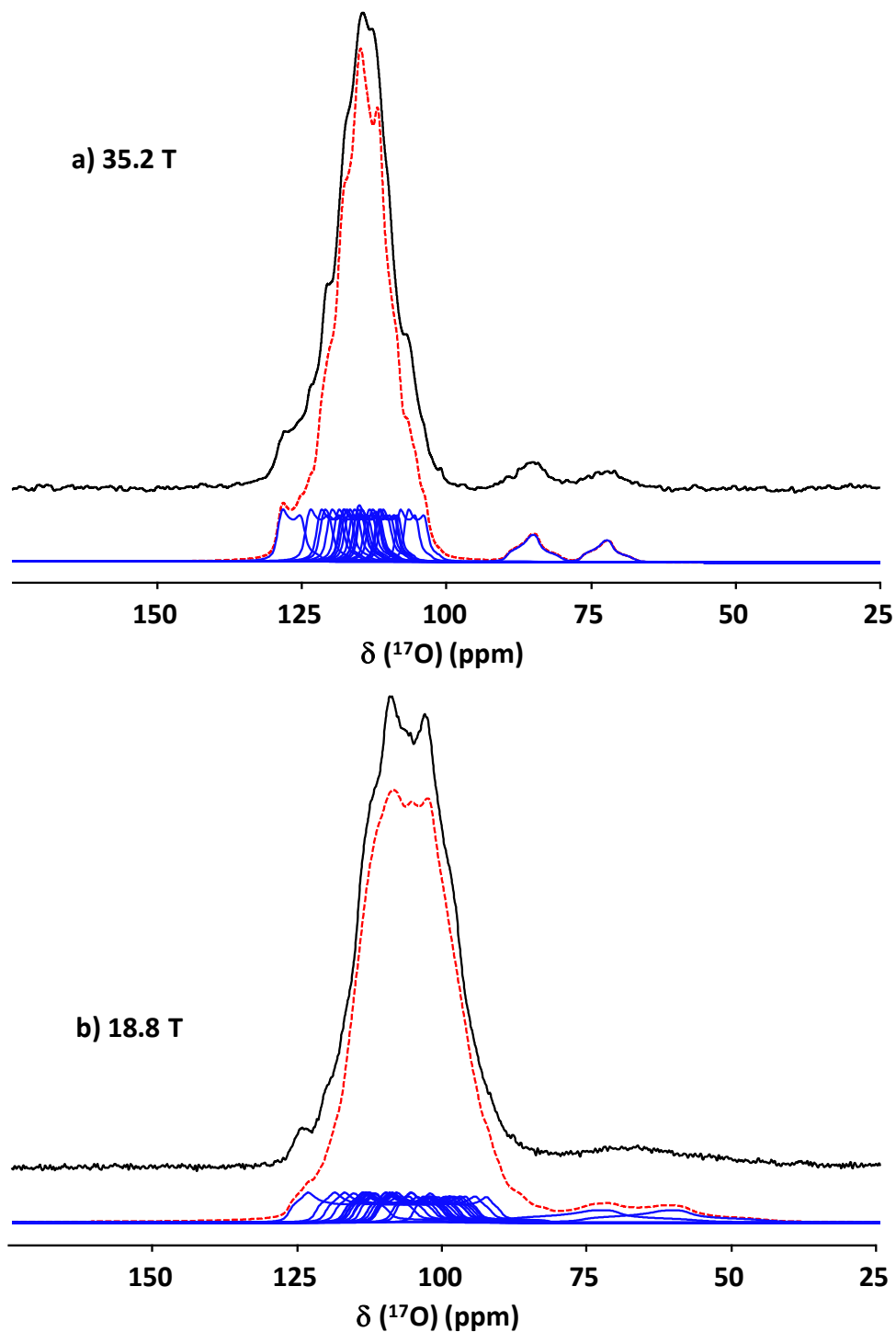


Figure S5: Experimental ^{43}Ca MAS NMR spectra of OCP recorded at ambient temperature: a) $B_0 = 35.2$ T, $v_r = 10$ kHz; b) $B_0 = 23.4$ T, $v_r = 40$ kHz c) $B_0 = 18.8$ T, $v_r = 8$ kHz (in black). A tentative fit is shown below each spectrum, with individual contributions of the Ca sites in blue, and their sum in red dashed line.

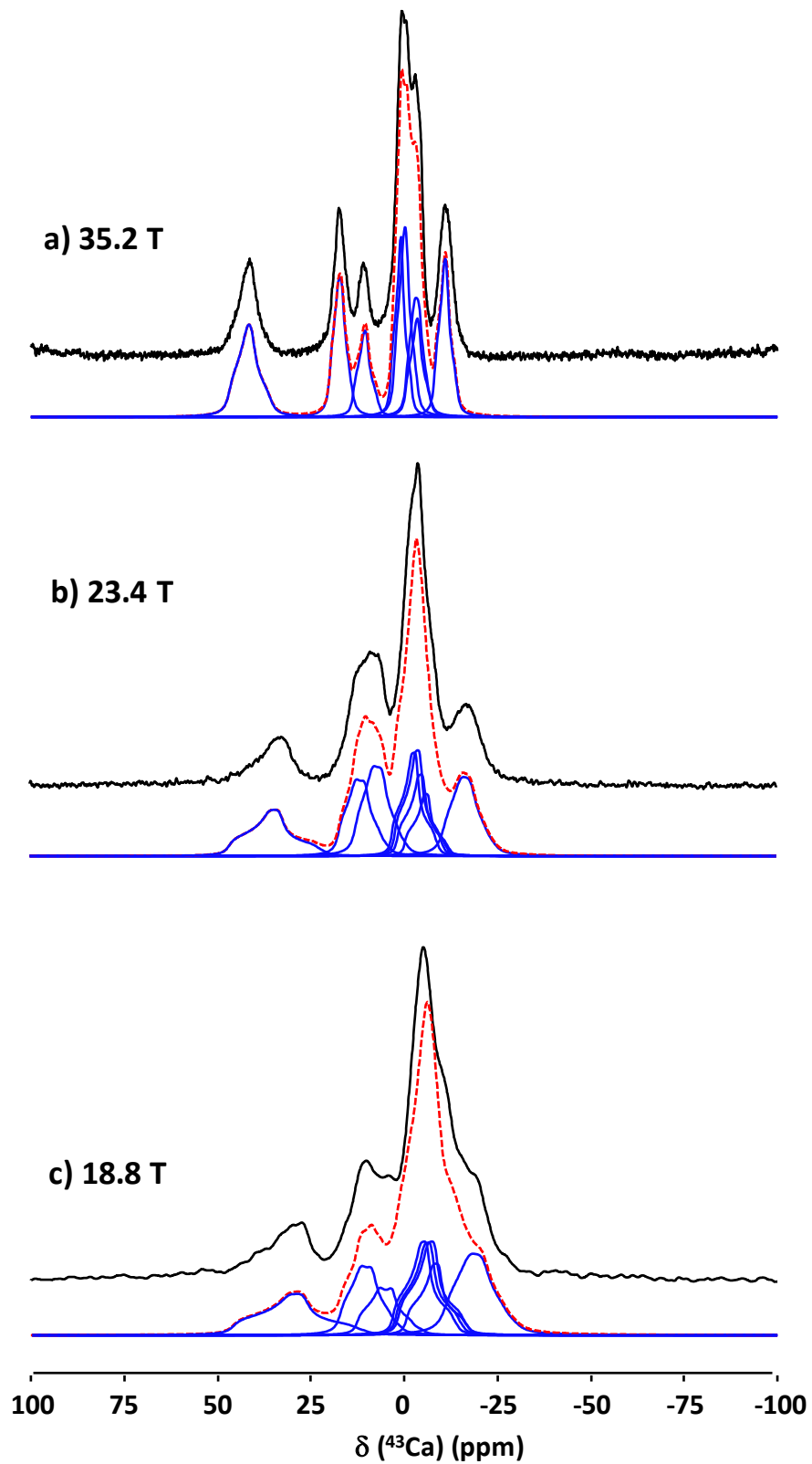


Figure S6: a) Staggered pXRD patterns obtained at variable temperatures, starting at 120 K, and increasing the temperature incrementally to 280 K. b) Same patterns but focussing on the 2θ region from 44° to 48° , to highlight the gradual shift of the diffraction peaks with temperature.

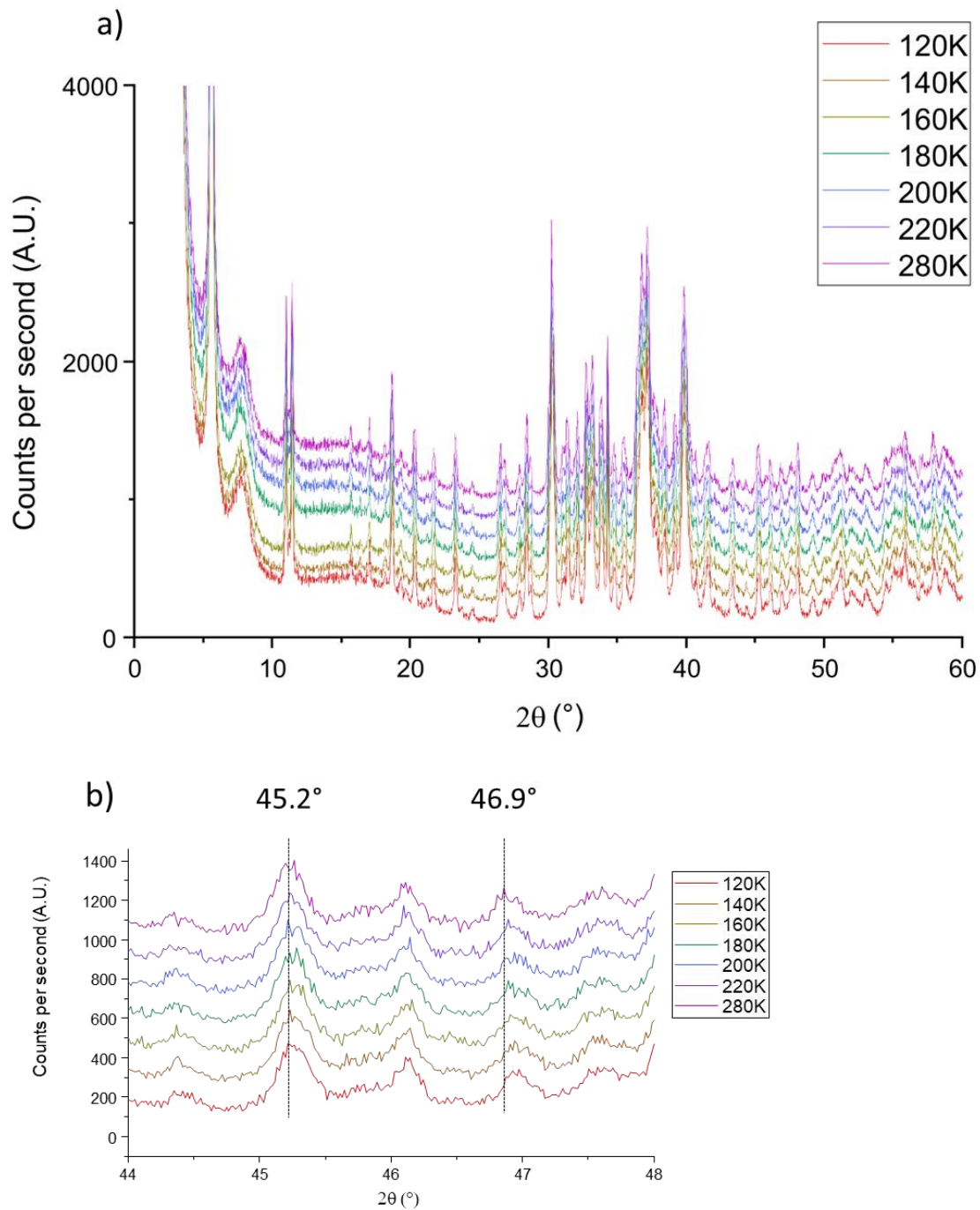


Figure S7: Evolution of the total energy of the molecular dynamics simulations over the length of the simulation, at a) 100 K and b) 300 K. c) Evolution of H-bonds starting from the central water molecules ($\text{H}_4\text{-O}23\text{-H}5$ and $\text{H}4'\text{-O}23'\text{-H}5'$) to the nearest HPO_4^{2-} ($\text{O}9'$ and $\text{O}9$), at 300 K, highlighting their “flipping” motion. Changes in configuration are noted by dotted vertical lines, and reproduced on b), showing that this motion has little noticeable effect on the overall energy of the structure.

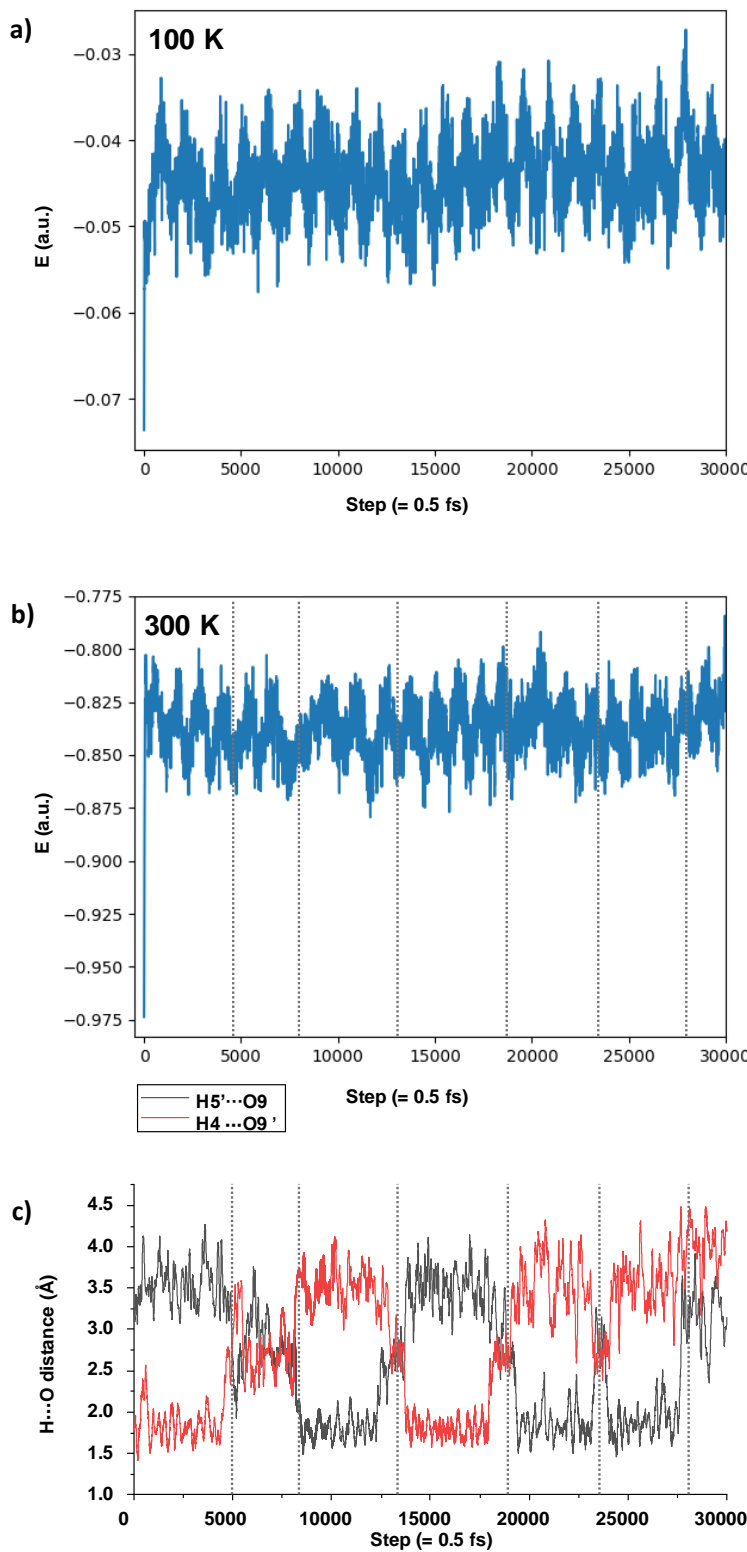


Figure S8: GIPAW calculated $\delta_{\text{iso}}(^{31}\text{P})$ of the P1 and P6 sites of OCP, along the MD simulation at a) 300 K and b) 100 K. Note the large variation of chemical shifts over the length of the simulation. Time-averaged $\delta_{\text{iso}}(^{31}\text{P})$ values at c) 300 K and d) 100 K.

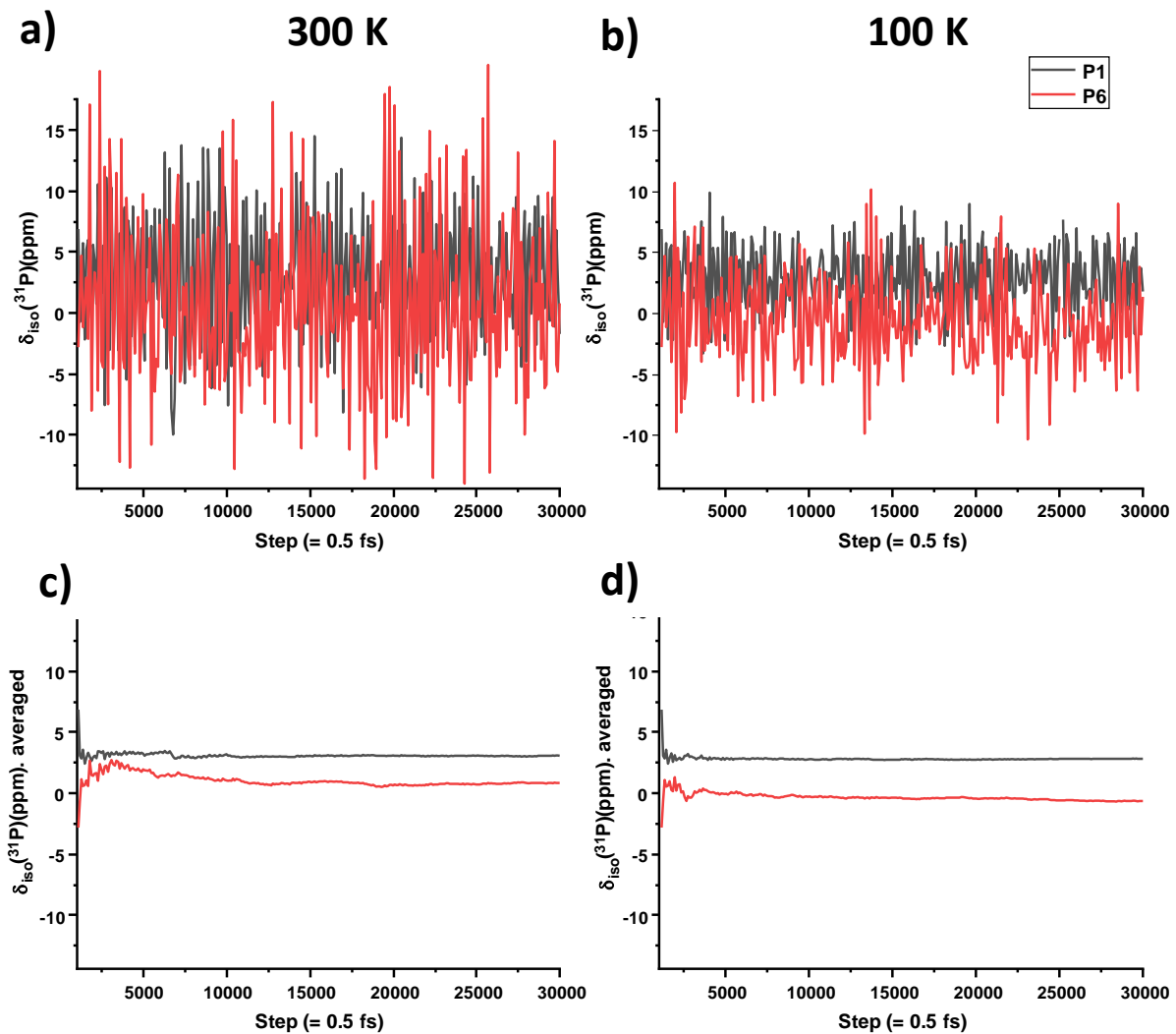


Figure S9: Experimental ^{43}Ca MAS NMR spectrum of OCP ($B_0 = 35.2$ T, $\nu_r = 10$ kHz, refrigerating unit set to 10°C) (in black), in comparison to the spectrum simulated based on DFT-GIPAW calculated parameters on the static relaxed structure² and after averaging by Molecular Dynamics at 300 K. Calculated contributions from Ca individual sites are shown below the spectra in red dashed line. It should be noticed that the referencing used for both calculations is a bit different.

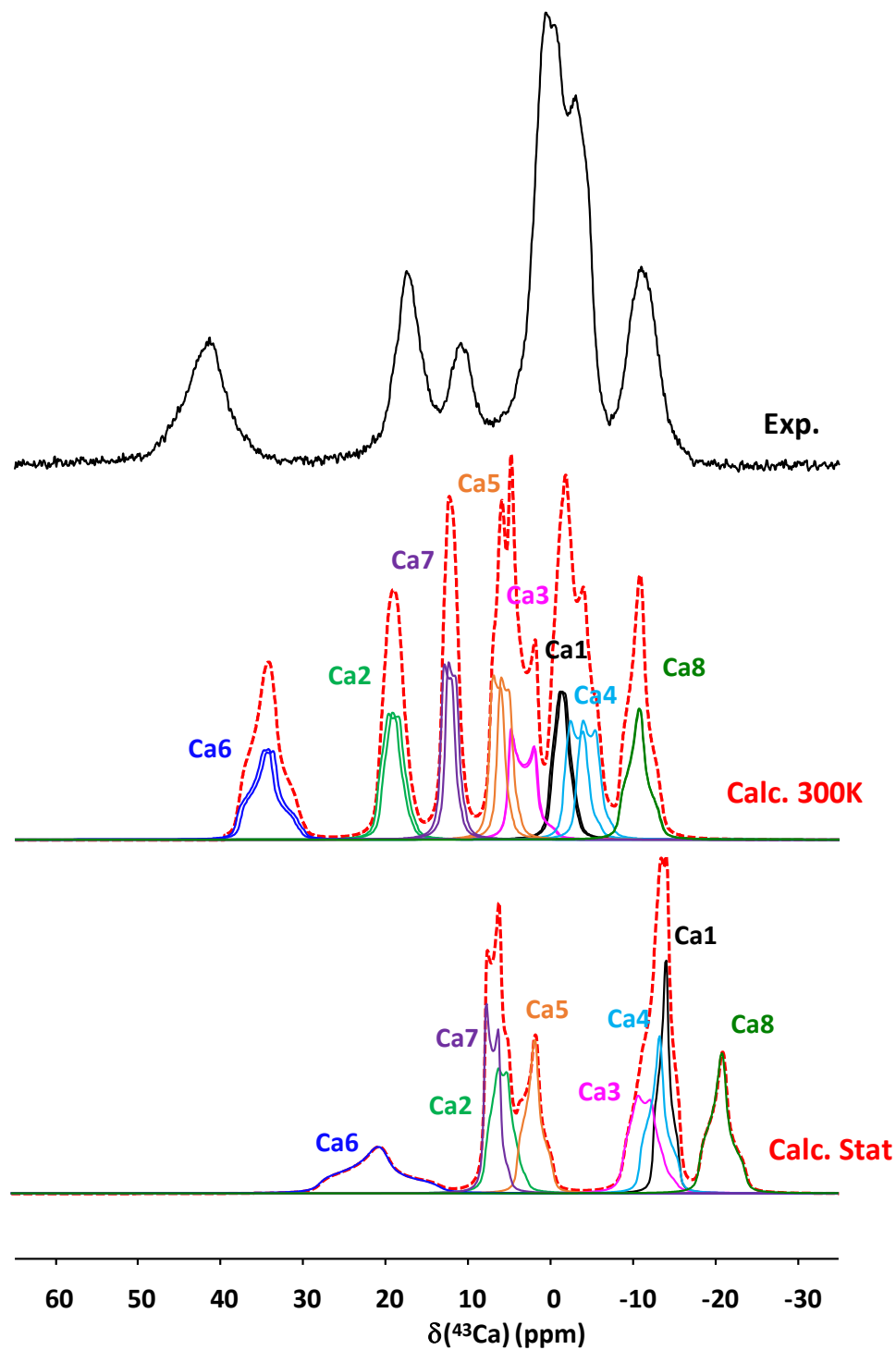


Figure S10: Calculated $\delta_{\text{iso}}(^{43}\text{Ca})$ for all calcium sites in OCP in the averaged MD structures for 300 K (red dots) and 100 K (blue square) simulations vs the average Ca---O distance for each Ca site (with a cut-off of 2.9 Å). In a number of previous studies, ${}^3\delta_{\text{iso}}(^{43}\text{Ca})$ could be related to a certain extent to the average Ca---O distance in the first coordination sphere of calcium. Here, data are scattered and no strong correlation can be established, apart from the fact that the most deshielded values tend to correspond to the shortest average Ca---O distances.

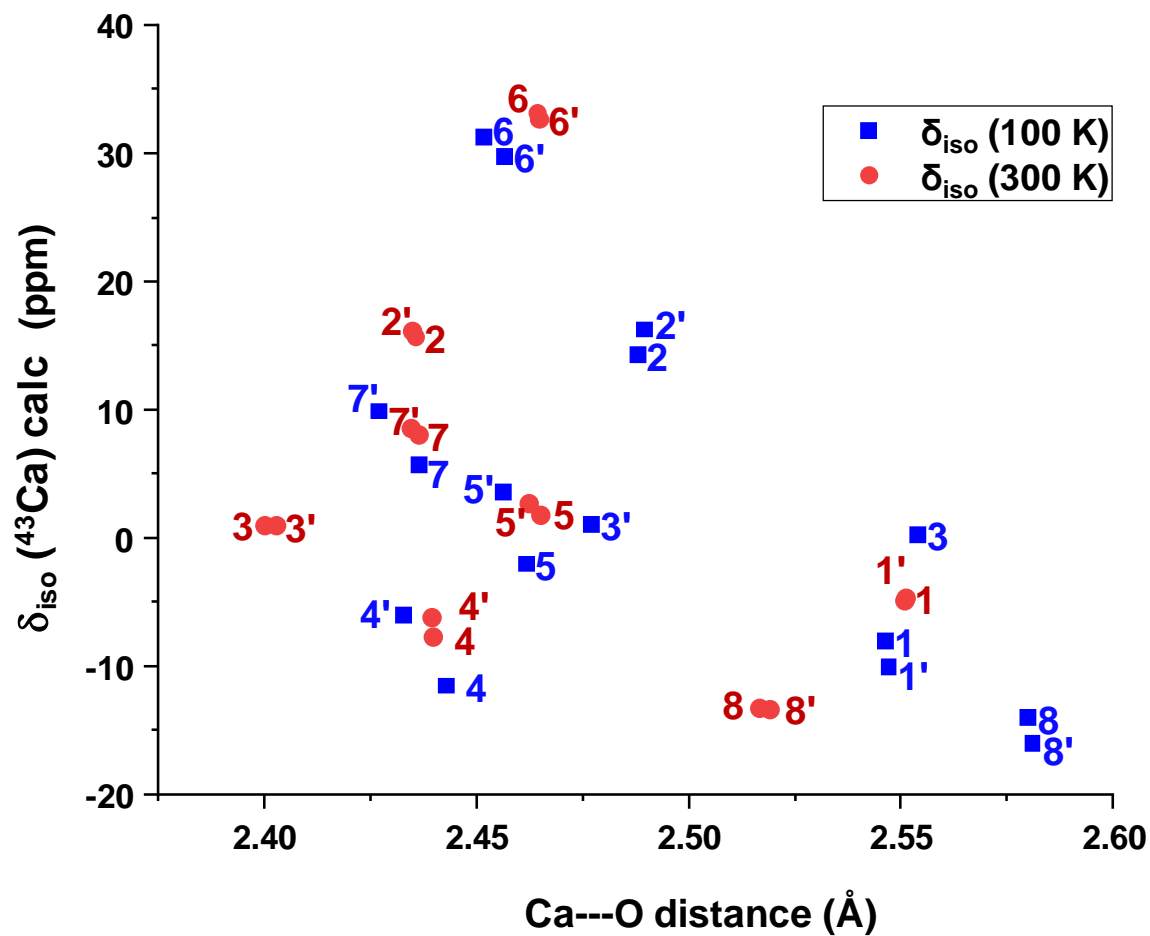


Figure S11: Comparison of the relative stability of H-bonds involving the P3 PO*H (O9) and the P6 PO*H (O15), over the a) 300 K MD simulation, and b) the 100 K MD simulation. The increased instability around P3 (in black) at 300 K may explain the lack of correlation between O9 and H1, whereas the O15-H6 correlation is visible (see D-RINEPT experiment in Figure 9). An inset illustrates the position of the relevant H-bonds within the structure.

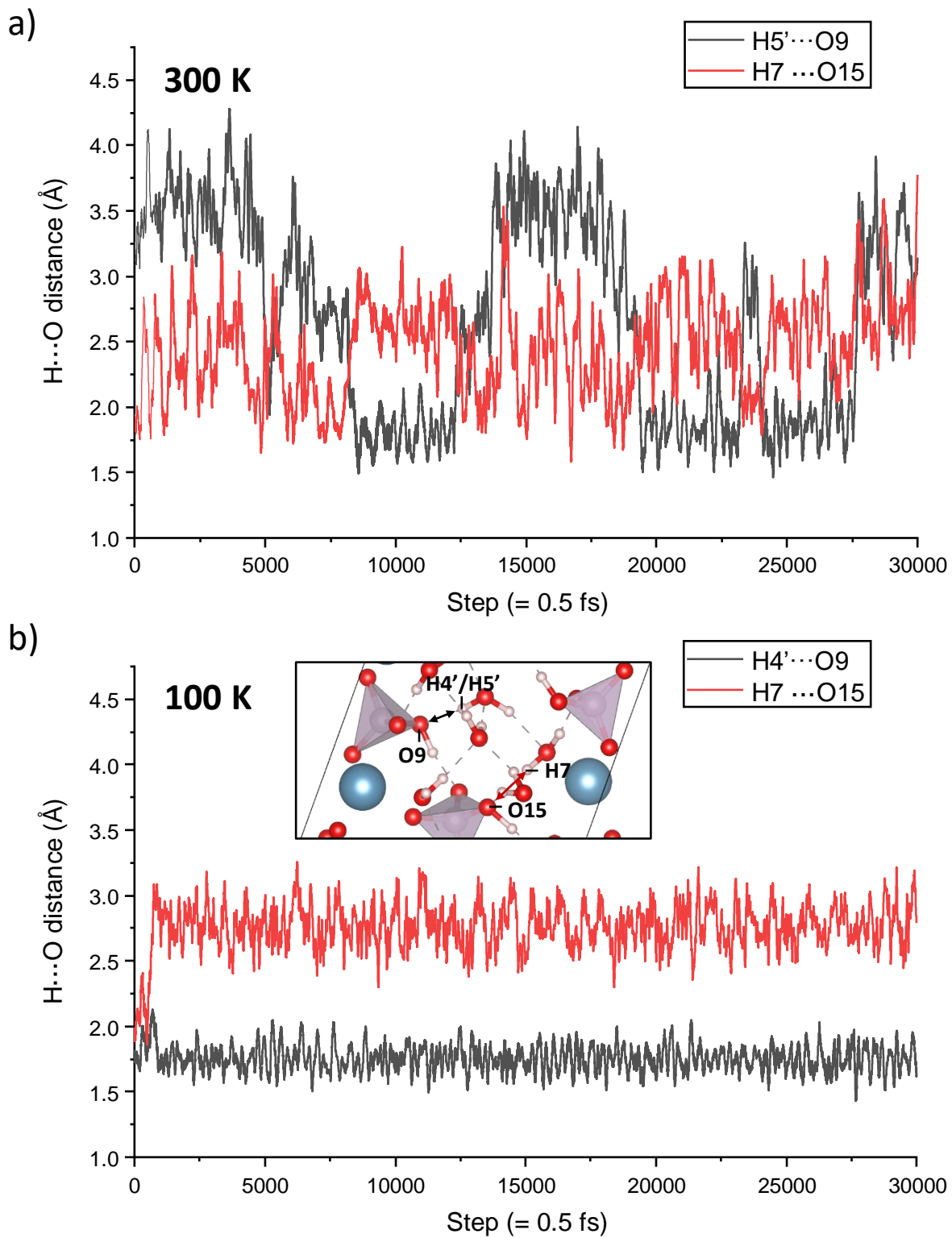


Figure S12: Calculated ^1H NMR chemical shifts plotted against the shortest $\text{O}-\text{H}\cdots\text{O}$ distances for the static relaxed structure (in green), and in the averaged MD structures at 300 K (in red) and 100 K (in blue). Note that POH and HOH (H-bond donors) are plotted with triangles and dots respectively.

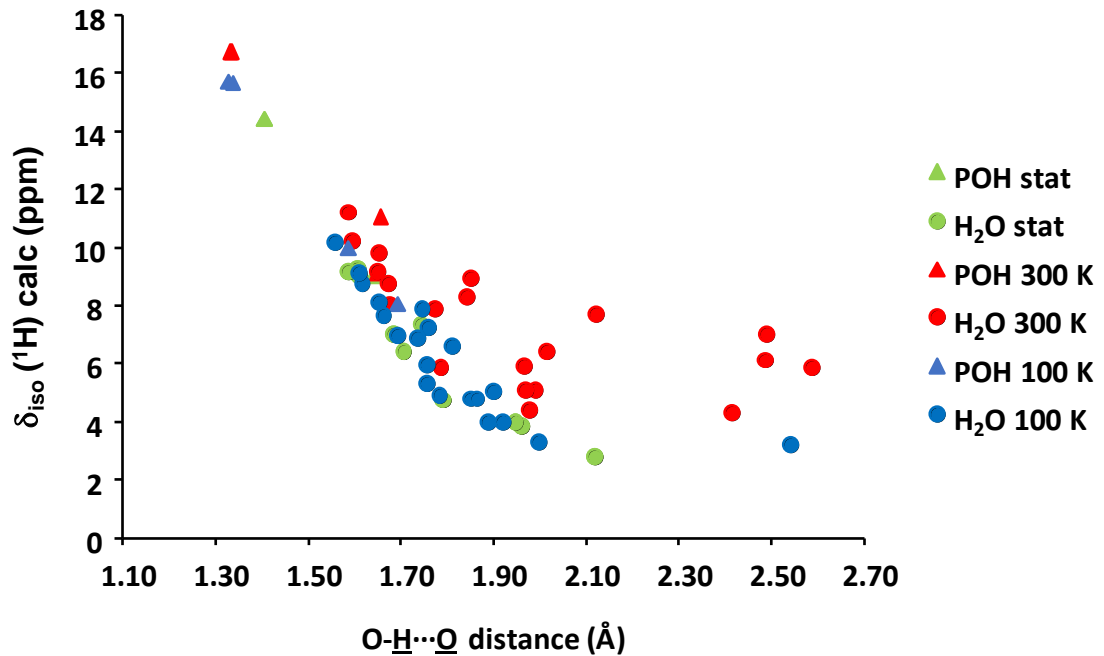


Figure S13: $\{^1\text{H}\} ^{31}\text{P}$ DNP S3 DQ/SQ correlation spectra recorded on unenriched OCP at ca. 100 K ($B_0 = 9.4$ T, $v_r = 10$ or 13 kHz) at three different recoupling times: a) 7.4 ms, b) 12.3 ms, c) 3.2 ms. The spectra show similar features at the different recoupling times (including very slight shifts in cross-peak positions, compared to the peak-maxima on the direct-excitation ^{31}P MAS NMR spectra, as mentioned in main text).

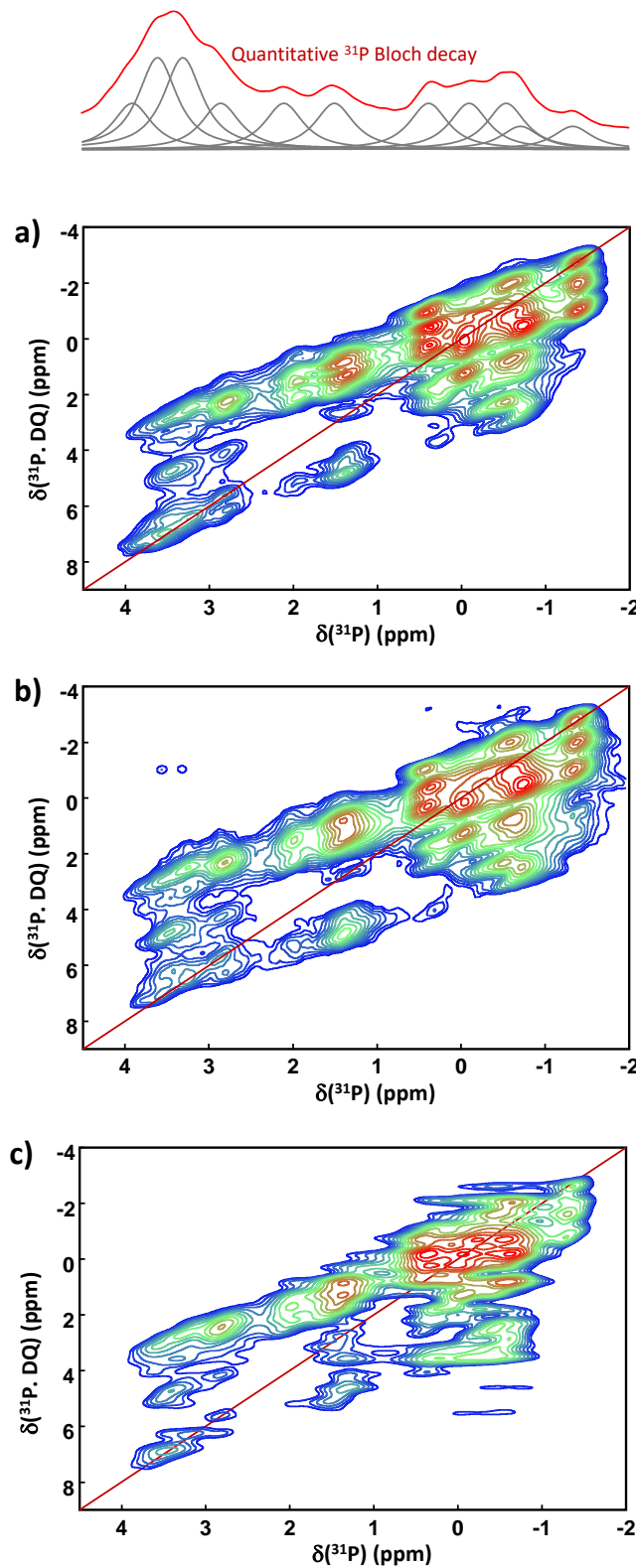
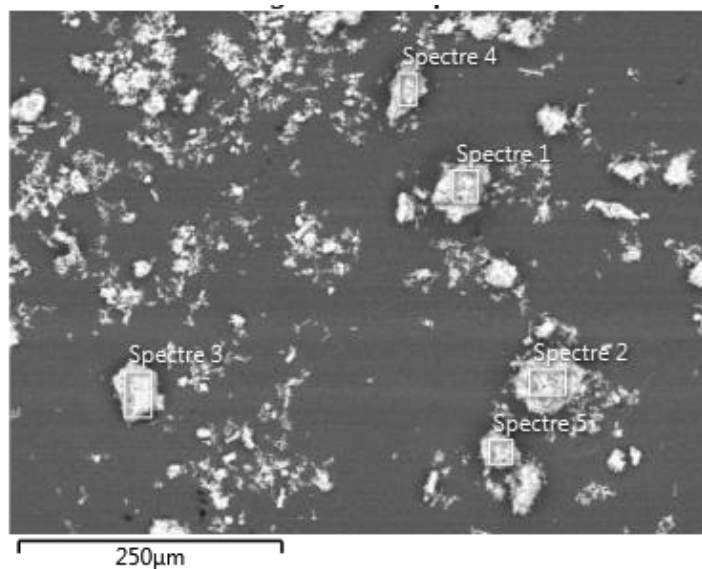


Table S1: EDXS analysis of gram-scale OCP, averaged over five spectra corresponding to different points of the sample.



	Spectrum 1	Spectrum 2	Spectrum 3	Spectrum 4	Spectrum 5
Ca/P molar ratio	1.42	1.37	1.34	1.55	1.38

Average Ca/P molar ratio	1.41 ± 0.06
--------------------------	-----------------

Table S2: ^{31}P experimental chemical shifts (extracted from NMR spectra recorded at ambient temperature and 100 K), and GIPAW-DFT calculated parameters (on the static relaxed structure, after extrapolation at 298 K,¹ and after averaging by Molecular Dynamics at 100 K or 300 K). Note that the two positions proposed for P3' at 100 K correspond to the assignment hypothesis *i)* and *ii)* discussed at the end of the main text.

Site	δ_{iso} (ppm)				
	Exp amb. (Fig 2a)	Exp 100 K (Fig 10b)	Stat calc ¹	300 K calc	100 K calc
P1	3.2	2.8	3.0	3.1	2.8
P1'	3.2	3.9	3.0	3.0	3.1
P2	2.0	3.5	1.9	1.2	0.7
P2'	2.0	3.2	1.9	1.1	0.6
P3	-0.3	1.4	-1.9	-2.7	-3.0
P3'	-0.3	-0.7/2.0	-1.9	-2.4	-2.2
P4	3.6	3.5	3.8	3.9	3.5
P4'	3.6	3.2	3.8	3.7	3.4
P5	-0.3	-1.3	-0.1	2.2	-0.4
P5'	-0.3	-0.2	-0.1	2.3	1.6
P6	-0.1	-0.6	0.7	0.8	-0.6
P6'	-0.1	0.3	0.7	0.2	0.1

Table S3: Experimental and fitted (Fig. S5) ^{43}Ca NMR parameters (recorded at ambient temperature), compared to the calculated values (on the static relaxed structure,² and after averaging by Molecular Dynamics at 100 K or 300 K).

Site	Site ²	δ_{iso} (ppm)				C_Q (MHz)				η_Q			
		Exp amb.	Stat calc ²	300K calc	100K calc	Exp amb. ^a	Stat calc ²	300K calc	100K calc	Exp amb.	Stat calc ²	300K calc	100K calc
Ca1	Ca1	-0.4	-12.6	0.3	-3.0	2.9	-2.2	-2.4	-2.7	0.8	0.9	0.6	0.5
Ca1'	Ca2	-0.4	-12.6	0.1	-5.6	2.9	-2.2	-2.4	-2.6	0.8	0.9	0.6	0.5
Ca2	Ca3	19.9	7.8	20.7	19.3	3.1	2.8	2.6	2.7	0.6	0.5	0.5	0.7
Ca2'	Ca4	19.9	7.8	21.2	21.3	3.1	2.8	2.6	2.8	0.6	0.5	0.5	0.7
Ca3	Ca5	2.6	-8.7	6.0	5.3	2.9	-3.2	-3.3	-3.3	0.8	0.5	0.0	0.2
Ca3'	Ca6	2.6	-8.7	5.9	6.1	2.9	-3.2	-3.3	-3.5	0.8	0.5	0.1	0.1
Ca4'	Ca7	-0.5	-11.0	-2.7	-6.5	2.8	-2.6	2.8	2.8	0.8	0.9	0.3	0.7
Ca4	Ca8	-0.5	-11.0	-1.2	-1.0	2.8	-2.6	2.8	2.8	0.8	0.9	0.3	0.5
Ca5	Ca9	3.5	3.8	6.8	4.8	2.8	-2.5	2.3	2.4	0.8	0.9	0.2	0.1
Ca5'	Ca10	3.5	3.8	7.7	8.6	2.8	-2.5	2.2	2.4	0.8	0.9	0.2	0.4
Ca6	Ca11	46.8	27.7	38.2	36.3	4.1	-4.6	-3.4	-3.4	0.8	0.9	0.8	0.7
Ca6'	Ca12	46.8	27.7	37.7	34.8	4.1	-4.6	-3.4	-3.5	0.8	0.9	0.7	0.7
Ca7	Ca13	13.6	8.2	13.1	10.7	3.1	-2.4	-2.1	-2.1	0.6	0.1	0.2	0.1
Ca7'	Ca14	13.6	8.2	13.6	14.9	3.1	-2.4	-2.2	-2.1	0.6	0.1	0.2	0.1
Ca8	Ca15	-8.2	-18.2	-8.3	-8.9	3.1	-2.8	2.7	2.8	0.6	0.9	0.8	0.9
Ca8'	Ca16	-8.2	-18.2	-8.3	-11.0	3.1	-2.8	2.7	2.7	0.6	0.9	0.8	0.8

^a Experimentally, only the absolute value of C_Q is extracted from the fitting (not its sign).

As some of the ^{43}Ca NMR lineshapes are featureless, it is difficult to determine precisely the quadrupolar parameters C_Q and η_Q . Therefore, quadrupolar parameter P_Q ($P_Q = C_Q \left(1 + \frac{\eta_Q^2}{3}\right)^{1/2}$) (1)

and δ_{iso} were also obtained for comparison by plotting (see graphs below) the position of the maximum of the peaks δ_{max} at each magnetic field against $1/(v_0)^2$ (where v_0 is the Larmor frequency of ^{43}Ca). P_Q and δ_{iso} were then derived using the equation $\delta_{\text{max}} = \delta_{\text{iso}} - 10^6 \left(\frac{1}{392}\right) \left(\frac{P_Q}{v_0}\right)^2$ (2).

	δ_{iso} (ppm)		P_Q (MHz)	
	From Fig. S5	From Eq. (2) and plot below	From Fig. S5 and Eq. (1)	From Eq. (2) and plot below
Ca1	-0.4	-1.9	3.2	2.1
Ca2	19.9	20.3	3.3	3.7
Ca3	2.6	3.0	3.2	3.4
Ca4	-0.5	-1.9	3.1	2.1
Ca5	3.5	3.0	3.1	3.0
Ca6	46.8	47.2	4.5	4.9
Ca7	13.6	13.7	3.3	3.4
Ca8	-8.2	-7.2	3.3	3.9

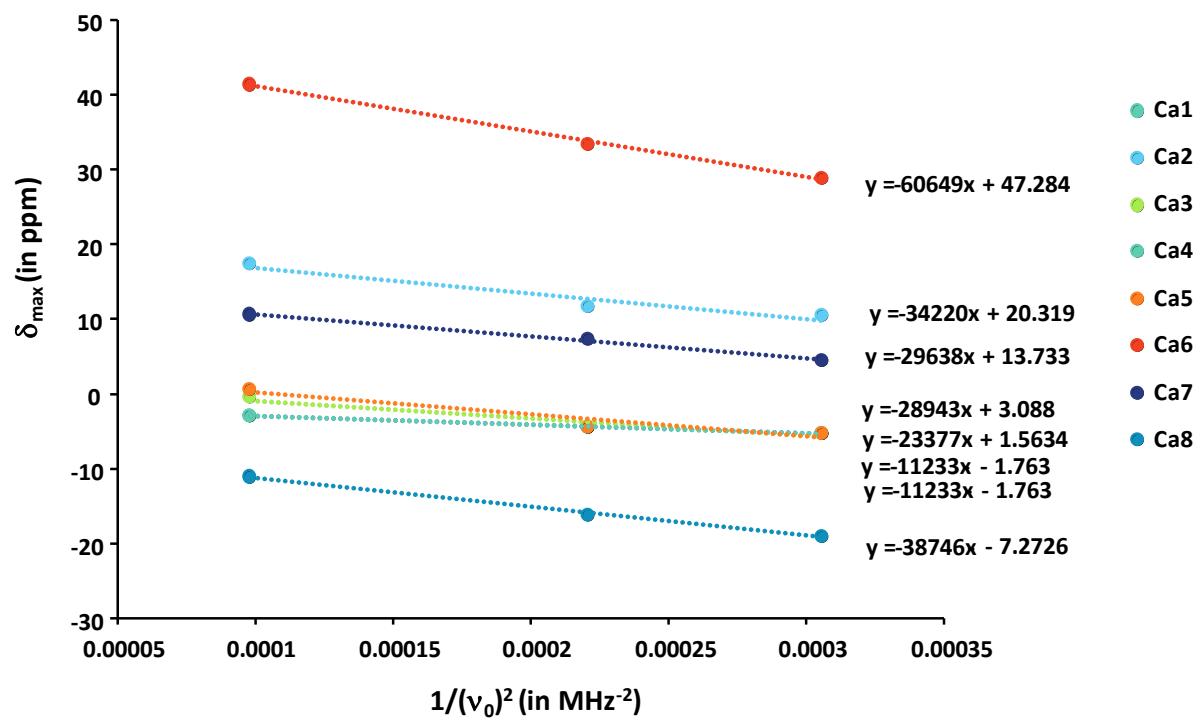


Table S4: ^{17}O experimental NMR parameters used for the tentative fit proposed on Figure S4.

Site	δ_{iso} (ppm)	C_Q (MHz)	η_Q
O15 (P-OH)	89.5	5.0	0.8
O9 (P-OH)	76.6	4.9	0.8
PO	129.9	4.8	0.2
	125.1	4.8	0.2
	123.2	4.8	0.2
	122.6	4.8	0.2
	121.4	4.8	0.2
	118.9	4.8	0.2
	120.2	4.8	0.2
	118.4	4.8	0.2
	119.4	4.8	0.2
	119.3	4.8	0.2
	117.6	4.8	0.2
	116.4	4.8	0.2
	116.9	4.8	0.2
	116.8	4.8	0.2
	114.5	4.8	0.2
	115.0	4.8	0.2
	113.0	4.8	0.2
	112.8	4.8	0.2
	112.3	4.8	0.2
	116.0	4.8	0.2
	109.3	4.8	0.2
	108.0	4.8	0.2

Table S5: Calculated ^1H NMR parameters and shortest OH---O distances on the static relaxed structure¹ and after time-averaging by Molecular Dynamics at 100 K and 300 K.

Site		δ_{iso} (Stat.) (ppm)	dOH---O (Å)	δ_{iso} (300K) (ppm)	dOH---O (Å)	δ_{iso} (100K) (ppm)	dOH---O (Å)
H1	POH	9.0	1.64	11.1	1.66	10.0	1.59
H1'	POH	9.0	1.64	9.1	1.65	8.1	1.69
H2	H_2O	7.4	1.75	9.0	1.85	7.9	1.75
H2'	H_2O	7.4	1.75	8.3	1.84	7.2	1.76
H3	H_2O	9.0	1.61	9.2	1.65	8.1	1.65
H3'	H_2O	9.0	1.61	9.8	1.66	8.7	1.62
H4	H_2O	4.7	1.79	6.1	2.49	5.0	1.91
H4'	H_2O	4.7	1.79	6.4	2.02	5.3	1.76
H5	H_2O	3.9	1.96	4.4	1.98	3.3	2.00
H5'	H_2O	3.9	1.96	5.9	2.59	4.8	1.86
H6	POH	14.4	1.41	16.8	1.33	15.7	1.33
H6'	POH	14.4	1.41	16.7	1.34	15.7	1.34
H7	H_2O	2.8	2.12	5.1	1.99	4.0	1.89
H7'	H_2O	2.8	2.12	5.1	1.97	4.0	1.92
H8	H_2O	9.3	1.61	11.2	1.59	10.2	1.56
H8'	H_2O	9.3	1.61	10.2	1.60	9.1	1.61
H9	H_2O	7.0	1.69	8.1	1.68	7.0	1.70
H9'	H_2O	7.0	1.69	8.7	1.68	7.7	1.66
H10	H_2O	9.2	1.59	7.9	1.78	6.8	1.74
H10'	H_2O	9.2	1.59	5.9	1.79	4.8	1.87
H11	H_2O	6.4	1.71	5.9	1.97	4.9	1.79
H11'	H_2O	6.4	1.71	7.0	2.49	6.0	1.76
H12	H_2O	4.0	1.95	7.7	2.12	6.6	1.81
H12'	H_2O	4.0	1.95	4.3	2.42	3.2	2.54

Table S6: Calculated ^{17}O NMR parameters on the static relaxed structure¹ and after time-averaging by Molecular Dynamics at 100 K and 300 K. Green highlight P-O*-H sites. H₂O oxygen sites are excluded.

	δ_{iso} (ppm)			C_{Q} (MHz)			η_{Q}		
Site	Stat calc	300K calc	100K calc	Stat calc	300K calc	100K calc	Stat calc	300K calc	100K calc
O1	108.5	123.2	120.8	-4.9	-5.0	-5.0	0.1	0.1	0.1
O1'	108.5	123.5	121.5	-4.9	-4.9	-5.0	0.1	0.1	0.1
O2	109.8	116.4	115.4	-5.4	-5.5	-5.6	0.2	0.3	0.3
O2'	109.8	116.4	113.9	-5.4	-5.5	-5.6	0.2	0.3	0.3
O3	122.5	135.0	134.0	-5.1	-5.4	-5.5	0.2	0.2	0.2
O3'	122.5	135.3	134.1	-5.1	-5.4	-5.5	0.2	0.2	0.2
O4	116.6	120.0	116.9	-5.2	-5.3	-5.4	0.1	0.2	0.2
O4'	116.6	119.1	115.3	-5.2	-5.3	-5.4	0.1	0.2	0.2
O5	112.0	124.6	121.0	-5.0	-5.2	-5.2	0.1	0.1	0.1
O5'	112.0	124.2	121.7	-5.0	-5.2	-5.2	0.1	0.1	0.1
O6	110.3	125.3	121.2	-5.2	-5.2	-5.3	0.1	0.1	0.1
O6'	110.3	124.8	122.2	-5.2	-5.2	-5.3	0.1	0.1	0.1
O7	126.1	133.4	130.9	-5.0	-5.2	-5.3	0.2	0.2	0.2
O7'	126.1	133.3	129.7	-5.0	-5.2	-5.3	0.2	0.2	0.2
O8	124.6	130.8	127.0	-4.9	-5.1	-5.2	0.2	0.2	0.2
O8'	124.6	130.2	127.1	-4.9	-5.1	-5.2	0.2	0.2	0.2
O9	64.2	71.5	74.6	-7.2	-6.9	-6.8	0.8	0.8	0.8
O9'	64.2	68.4	58.6	-7.2	-7.0	-7.4	0.8	0.9	1.0
O10	105.6	110.7	110.5	-5.1	-5.1	-5.2	0.2	0.1	0.2
O10'	105.6	110.5	108.1	-5.1	-5.1	-5.3	0.2	0.1	0.2
O11	108.4	124.3	115.0	-5.2	-5.3	-5.4	0.1	0.1	0.1
O11'	108.4	126.2	124.1	-5.2	-5.3	-5.5	0.1	0.1	0.1
O12	116.9	129.8	127.1	-5.0	-5.1	-5.2	0.1	0.2	0.2
O12'	116.9	130.0	128.6	-5.0	-5.2	-5.2	0.1	0.2	0.2
O13	119.3	129.8	127.6	-5.3	-5.4	-5.4	0.1	0.1	0.1
O13'	119.3	129.1	126.1	-5.3	-5.3	-5.4	0.1	0.1	0.1
O14	103.5	121.5	114.8	-5.1	-5.3	-5.3	0.2	0.2	0.2
O14'	103.5	120.8	114.5	-5.1	-5.3	-5.4	0.2	0.2	0.2
O15	73.7	88.3	83.2	-6.4	-6.1	-6.4	0.8	0.7	0.7
O15'	73.7	88.0	85.9	-6.4	-6.2	-6.2	0.8	0.7	0.8
O16	95.5	104.9	103.9	-5.3	-5.3	-5.3	0.3	0.3	0.3
O16'	95.5	103.7	100.1	-5.3	-5.4	-5.5	0.3	0.3	0.2
O17	127.9	141.5	140.0	-5.3	-5.4	-5.5	0.2	0.1	0.1
O17'	127.9	141.7	138.9	-5.3	-5.4	-5.5	0.2	0.1	0.1
O22	121.3	130.3	128.1	-5.1	-5.3	-5.3	0.1	0.1	0.1
O22'	121.3	130.2	128.8	-5.1	-5.3	-5.4	0.1	0.1	0.1
O24	126.3	129.7	125.5	-4.8	-5.0	-5.1	0.0	0.1	0.1
O24'	126.3	129.9	127.2	-4.8	-5.0	-5.1	0.0	0.1	0.1
O25	117.7	128.9	127.1	-5.0	-5.0	-5.1	0.0	0.1	0.1
O25'	117.7	128.8	126.1	-5.0	-5.1	-5.1	0.0	0.1	0.1
O26	116.3	130.0	126.4	-4.9	-5.1	-5.1	0.0	0.1	0.1
O26'	116.3	130.5	125.6	-4.9	-5.0	-5.1	0.0	0.0	0.1

O27	140.2	147.6	146.7	-5.0	-5.2	-5.2	0.1	0.1	0.1
O27'	140.2	147.8	145.2	-5.0	-5.2	-5.2	0.1	0.1	0.1
O28	105.8	113.9	110.3	-5.2	-5.3	-5.4	0.1	0.1	0.1
O28'	105.8	114.1	112.1	-5.2	-5.3	-5.4	0.1	0.1	0.1
O29	115.5	126.6	123.9	-5.1	-5.3	-5.4	0.2	0.1	0.2
O29'	115.5	127.4	125.3	-5.1	-5.3	-5.4	0.2	0.1	0.1

Table S7: Selected Ca...H distances (shorter than 3.40 Å) for all crystallographically inequivalent calcium sites in the structure averaged by MD at 300 K.

Ca7	H3	2.73
Ca7'	H3'	2.74
Ca5'	H3'	2.78
Ca5	H3	2.78
Ca7	H9	2.85
Ca7'	H9'	2.85
Ca4	H12	2.86
Ca4'	H12'	2.87
Ca7	H6	2.90
Ca7'	H6'	2.91
Ca3	H9	2.95
Ca3'	H9'	2.96
Ca5'	H2'	2.99
Ca5	H2	3.00
Ca3'	H8'	3.01
Ca3	H8	3.01
Ca3	H7	3.02
Ca3'	H7'	3.03
Ca7	H2	3.04
Ca7'	H2'	3.04
Ca4	H11	3.12
Ca4'	H11'	3.14
Ca3	H10	3.15
Ca3'	H10'	3.16
Ca7'	H10'	3.18
Ca7	H10	3.19
Ca8'	H3'	3.31
Ca8	H3	3.31
Ca6'	H3'	3.36
Ca6	H3	3.36
Ca8	H6	3.38
Ca8'	H6'	3.38

Table S8: ^{31}P resonances extracted from the simulation of the quantitative 1D NMR spectrum (Fig 10b), with chemical shift, linewidth and integration. Total sum of integrals is 12. Note that the two possible assignments of sites correspond to hypothesis *i*) and *ii*) discussed at the end of the main text.

Site <i>i</i>)	Site <i>ii</i>)	$\delta_{\text{iso}}^{\text{exp}}$ (ppm)	FWHM (ppm)	Integration (a.u.)
P5	P5	-1.3	0.55	0.5
P3'	P°	-0.7	0.55	0.5
P6	P6	-0.6	0.55	1.0
P5'	P5'	-0.2	0.55	1.0
P6'	P6'	0.3	0.55	1.0
P3	P3	1.4	0.55	1.0
P*	P3'	2.0	0.55	1.0
P1	P1	2.8	0.55	1.0
P2'/P4'	P2'/P4'	3.2	0.55	2.0
P2/P4	P2/P4	3.5	0.55	2.0
P1'	P1'	3.9	0.55	1.0

Table S9: Characteristic CP dynamics parameters obtained by fitting the amplitude of different components of the ^{31}P CPMAS NMR spectra of unenriched OCP at ca. 100 K (Fig. 11).

$\delta_{\text{iso}}(^{31}\text{P})$ (ppm)	I_0 (a.u.)	T_{cp} (ms)	$T_{1\rho}$ (ms)	R^2
-1.3	36.9 ± 0.2	0.41 ± 0.01	9.1 ± 0.2	0.9964
-0.7	63.5 ± 0.5	0.31 ± 0.01	3.4 ± 0.1	0.9959
-0.6	81.3 ± 0.9	0.80 ± 0.01	18.9 ± 1.3	0.9972
-0.2	74.8 ± 0.5	0.44 ± 0.01	14.5 ± 0.5	0.9953
0.3	78.5 ± 0.7	0.53 ± 0.01	23.5 ± 1.5	0.9951
1.4	79.4 ± 0.4	0.30 ± 0.01	32.6 ± 1.7	0.9949
2.0	30.1 ± 0.1	1.80 ± 0.01	>> 50	0.9997
2.8	39.4 ± 0.2	1.11 ± 0.02	>> 50	0.9958
3.2	32.7 ± 0.2	3.36 ± 0.04	>> 50	0.9995
3.5	46.6 ± 0.3	2.03 ± 0.03	>> 50	0.9982
3.9	48.2 ± 0.5	3.86 ± 0.07	>> 50	0.9991

Table S10: Distances between phosphorus sites to their nearest proton site in the 100 K averaged MD structure.

Site	P1	P2	P3	P4	P5	P6
Nearest proton	H3	H2	H6	H3	H1	H6
Distance (Å)	4.4	3.4	2.4	3.9	2.2	2.3
Next nearest	H2	H11	H7	H2	H4'	H3 & H1
Distance (Å)	5.2	3.8	3.3	4.6	2.7	2.6
Site	P1'	P2'	P3'	P4'	P5'	P6'
Nearest proton	H3'	H2'	H6'	H3'	H1'	H6'
Distance (Å)	4.3	3.4	2.4	3.9	2.2	2.3
Next nearest	H2'	H11'	H7'	H2'	H8	H3' & H1'
Distance (Å)	5.2	3.8	3.3	4.6	2.7	2.6 & 2.7

References

- [1] E. Davies, M. J. Duer, S. E. Ashbrook and J. M. Griffin, *J. Am. Chem. Soc.*, 2012, **134**, 12508–12515.
- [2] D. Laurencin, Y. Li, M. J. Duer, D. Iuga, C. Gervais and C. Bonhomme, *Magn. Reson. Chem.*, 2021, **59**, 1048–1061.
- [3] C. Gervais, D. Laurencin, A. Wong, F. Pourpoint, J. Labram, B. Woodward, A. P. Howes, K. J. Pike, R. Dupree, F. Mauri, C. Bonhomme and M. E. Smith, *Chem. Phys. Lett.*, 2008, **464**, 42–48.